

Cost-efficient RIS-assisted Transmitter Design with Discrete Phase Shifts for Wireless Communication

Xiangyu Pi, Pengfei Yi, *Graduate Student Member, IEEE*, Zhenyu Xiao, *Senior Member, IEEE*, Wei Zhang, *Fellow, IEEE*, Zhu Han, *Fellow, IEEE*, and Xiang-Gen Xia, *Fellow, IEEE*

Abstract—In this letter, in order to achieve higher spectral and energy efficiency, we propose a novel cost-efficient transmitter conceptual design based on reconfigurable intelligent surface (RIS) with discrete phase shifts. The key idea is to directly utilize the digital signal to adjust the discrete reflection coefficients of RIS, resulting that the phases of the reflected carrier signal being modulated without the need for complex digital signal processing (DSP) hardware and costly radio frequency (RF) chains. Furthermore, a joint digital modulation and beamforming method is developed to enable information transmission as well as enhance signal strength. Based on the proposed transmitter, we derive the closed-form expressions of the signal-to-noise ratio (SNR) and bit error rate (BER) of the received signal and analyze the impact of hardware constraints on communication performance. Extensive simulation results validate that the novel design of RIS-assisted transmitter provides a cost-effective and power-efficient solution for wireless communications.

Index Terms—Reconfigurable intelligent surface (RIS), transmitter, cost efficiency, digital modulation.

I. INTRODUCTION

IN order to support the extremely high access rate and superior network capacity in the future wireless communication systems, various key technologies, such as massive multiple-input multiple-output (MIMO), millimeter-wave (mmWave), Terahertz (THz), and ultra-dense network are under active discussion. However, conventional multi-antenna transceivers have high hardware cost and energy consumption, because complex digital signal processing (DSP) hardware is required to achieve information transfer, and a large number of radio-frequency (RF) chains and phase antenna arrays are needed to obtain high array gain [1]. As a result, there is an urgent need to develop cost-effective and power-efficient new transceiver architectures to support the practical application of these emerging technologies.

This work was supported in part by the National Natural Science Foundation of China (NSFC) under grant numbers 62171010, U22A2007 and 61827901, and the Beijing Natural Science Foundation under grant number L212003, and in part by NSF CNS-2107216, CNS-2128368, CMMI-2222810, Toyota and Amazon. (*Corresponding author: Zhenyu Xiao.*)

X. Pi, P. Yi, and Z. Xiao are with the School of Electronic and Information Engineering, Beihang University, Beijing 100191, China. (pixiangyu@buaa.edu.cn, yipengfei@buaa.edu.cn, xiaozy@buaa.edu.cn)

W. Zhang is with the School of Electrical Engineering and Telecommunications, the University of New South Wales, Sydney, NSW 2052, Australia. (e-mail: w.zhang@unsw.edu.au)

Z. Han is with the Department of Electrical and Computer Engineering at the University of Houston, Houston, TX 77004 USA, and also with the Department of Computer Science and Engineering, Kyung Hee University, Seoul, South Korea, 446-701. (zhan2@uh.edu)

X.-G. Xia is with the Department of Electrical and Computer Engineering, University of Delaware, Newark, DE 19716, USA. (xianggen@udel.edu)

Recently, reconfigurable intelligent surface (RIS) has drawn significant attention due to the potential to achieve high spectrum efficiency and energy efficiency simultaneously [2], [3]. RIS is a planar array architecture composed of a large number of passive elements, which can independently reflect electromagnetic waves and flexibly adjust their amplitudes and/or phases. Apart from the widely studied scenarios of deploying RIS as a passive relay to control the propagation environment to increase the quality of service (QoS) and/or achieve coverage enhancement [4]–[6], there are growing interests on utilizing RISs to implement transmitters with low power consumption and hardware cost. On one hand, by intelligently manipulating signals to reconfigure them toward their desired directions, the energy-efficient RIS is chosen to replace the energy-hungry phased antenna array to perform analog beamforming (ABF) in [7] and [8]. However, the above works focused on the RIS-aided hybrid precoding schemes in which the digital baseband modulation relies on DSP hardware and multiple RF chains, resulting in an additional hardware overhead. On the other hand, there are a few works for utilizing RISs to reflect the unmodulated carrier signal with adjustable phase shifts to achieve RF chain-free modulation. The works [9] and [10] proposed using RIS to realize frequency-shift keying (FSK) modulation and quadrature phase-shift keying (QPSK) modulation, respectively. Furthermore, utilizing RIS to achieve quadrature amplitude modulation (QAM) and to facilitate the implementation of MIMO transmission was proposed in [11]. However, RISs used in these works on RIS-based modulation are made of varactors and continuous phase shifts are achieved at each reflecting element, which is costly for practical implementation due to the hardware limitation. In addition, a large number of digital-to-analog converters (DACs) are required to convert the digital baseband signal into a control signal, to adjust the reflection phases of the RIS. Therefore, compared to the conventional transmitters, the existing RIS-based transmitters do not have significant advantages in terms of hardware complexity.

Different from the above works, in this letter, we propose a cost-efficient RIS-assisted transmitter design with discrete phase shifts for wireless communication. First, we propose a novel direct digital modulation (DDM) method based on discrete-phase RIS, which directly utilizes the digital signal to adjust the reflection coefficients of RIS to achieve M -ary phase shift keying (MPSK) modulation. In addition, we provide the method of joint digital modulation and analog beamforming to convey information and enhance signal strength without the need for DSP hardware or multiple RF chains. Moreover,

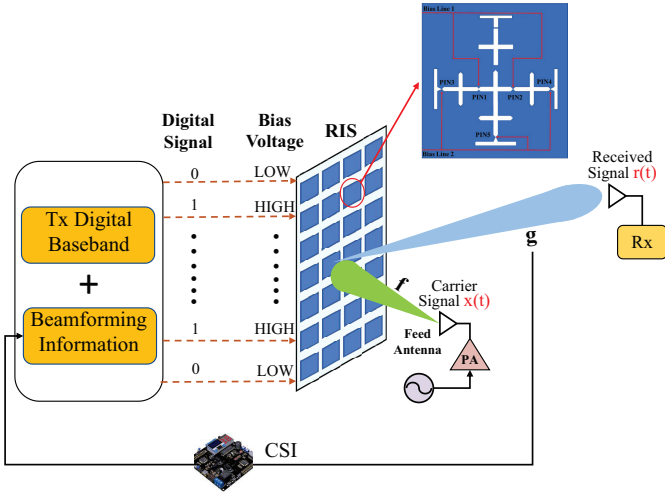


Fig. 1. MISO system based on cost-efficient RIS-assisted transmitter.

we derive the closed-form expressions of signal-to-noise ratio (SNR) and bit error rate (BER) performance and analyze the impact of the number of reflecting elements and the phase quantization levels on the performance. Finally, simulation results show that the proposed transmitter is capable of approaching the performance of conventional transmitters or existing RIS-based transmitters with lower hardware complexity and energy consumption.

The remaining of this letter is organized as follows. Section II presents the system model. The signal demodulation and performance analysis are given in Section III, and the simulation results are detailed in Section IV. Finally, conclusions are provided in Section V.

II. SYSTEM MODEL

A. Signal Model

A RIS-assisted multiple-input single-output (MISO) wireless communication system, where the RIS is effectively used as a passive reflector with a feed antenna at the transmitter (Tx) side and a single antenna is placed at the receiver (Rx) side, is considered in this letter and illustrated in Fig 1. The single carrier signal $x(t)$ transmitted by the feed antenna travels through channel $\mathbf{f} \in \mathbb{C}^{N \times 1}$ to the RIS which consists of N reflecting elements. After the phase shifting induced by the RIS, the reflected signal is received by the Rx through channel $\mathbf{g} \in \mathbb{C}^{N \times 1}$. Thus, in a symbol duration, the received signal at the Rx side can be written as

$$r(t) = \mathbf{g}^H \Theta \mathbf{f} x(t) + w(t) = \sqrt{P} \mathbf{g}^H \Theta \mathbf{f} e^{2\pi f_c t} + w(t), \quad (1)$$

where $x(t) = \sqrt{P} e^{2\pi f_c t}$, P is the transmit power of the feed antenna, f_c is the carrier frequency and $w(t)$ is additive white Gaussian noise (AWGN) at the Rx side. Θ is the reflection coefficient diagonal matrix of the RIS, which can be expressed as

$$\Theta = \text{diag}\{e^{j\theta_1}, \dots, e^{j\theta_n}, \dots, e^{j\theta_N}\} \in \mathbb{C}^{N \times N}, \quad (2)$$

where $\theta_n \in [0, 2\pi)$ is the phase shift reflection coefficient of the n -th element of RIS.

We assume that the feed antenna directly illuminates the RIS and perpendicularly transmit a planar-wave under the far-field condition. In addition, there is no obstacle between the feed antenna and the RIS. Thus, the channel from the feed antenna to RIS \mathbf{f} can be treated as a deterministic line-of-sight (LOS) channel

$$\mathbf{f} = \sqrt{\rho d^{-2}} [e^{-j\frac{2\pi}{\lambda}d}, \dots, e^{-j\frac{2\pi}{\lambda}d}, \dots, e^{-j\frac{2\pi}{\lambda}d}]^T, \quad (3)$$

where ρ is the path loss at the reference distance of 1 meter (m), d is the distance between the center of the RIS and the feed antenna, and λ is the carrier wavelength. Considering a downlink communication scenario with dense obstacles, the channel \mathbf{g} from the RIS to the Rx can be modeled as an independent and identically distributed (i.i.d.) Rayleigh fading channel

$$\mathbf{g} = \sqrt{\rho D^{-\alpha}} [|g_1|e^{j\beta_1}, \dots, |g_n|e^{j\beta_n}, \dots, |g_N|e^{j\beta_N}]^T, \quad (4)$$

where D is the distance between the RIS and user, and α is the path loss exponent. Its entries are i.i.d. complex Gaussian random variables with zero mean and unit variance, i.e., $|g_n|e^{j\beta_n} \sim \mathcal{CN}(0, 1)$. Therefore, the cascaded channel from the feed antenna to RIS and then to Rx can be expressed as

$$\mathbf{h} = \mathbf{g}^H \mathbf{F} = \eta [|h_1|e^{j\phi_1}, \dots, |h_n|e^{j\phi_n}, \dots, |h_N|e^{j\phi_N}], \quad (5)$$

where \mathbf{F} is a diagonal matrix whose diagonal elements are the elements of vector \mathbf{f} , $\eta = \rho\sqrt{d^{-2}D^{-\alpha}}$ represents the path loss, and $|h_n|e^{j\phi_n} = |g_n|e^{-j(\beta_n - \frac{2\pi}{\lambda}d)}$ follows the same distribution with $|g_n|e^{j\beta_n}$.

Therefore, the received signal in (1) can be rewritten as

$$r(t) = \mathbf{h} \boldsymbol{\theta} x(t) + w(t). \quad (6)$$

where $\boldsymbol{\theta} \in \mathbb{C}^{N \times 1}$ is the vector consisting of the diagonal elements of the reflection coefficient matrix Θ .

B. Direct Digital Modulation

As illustrated in the upper right of Fig. 1, the reflecting elements of the RIS are made of positive intrinsic-negative (PIN) diodes whose switching states are controlled by the bias voltage on the bias lines. Moreover, by changing the bias voltage and turning ON or OFF the PIN diodes, the phase shifts of reflecting elements can be discretely adjusted. For example, 2 bias lines and 5 PIN diodes can obtain four element phase states which clearly exhibit a 2-bit phase resolution with an approximate phase increment of 90° [12]. The higher phase resolution can also be realized by implementing more PIN diodes and bias lines. Based on the unique RIS structure, we propose using the digital signal composed of digital baseband and beamforming information directly as the bias voltage on the bias line, without the need for DACs to convert the digital signals into analog control signals. The set of digital signals to control each reflecting element can be denoted as

$$\mathcal{D} = \left\{ \underbrace{00 \cdots 0, 00 \cdots 1, \dots, 11 \cdots 1}_{b\text{-bits}} \right\}, \quad (7)$$

whose corresponding set of phase shifts at the reflecting elements is

$$\mathcal{R} = \left\{ 0, \frac{2\pi}{K}, \dots, \frac{K-1}{K}2\pi \right\}, \quad (8)$$

where $K = 2^b$ is the phase quantization levels. For the sake of representation, we denote the RIS with 2^b phase states as b -bit RIS. As can be seen, bN -bits digital signals are needed to control an RIS with N reflecting elements. Furthermore, the digital control signals to control the RIS can be uniquely determined by the desired reflection coefficients.

The function of adjusting the reflection coefficients of the RIS is to accomplish digital baseband modulation and achieve analog beamforming. Thus, the digital control signal which can adjust the reflection phase of RIS is composed of the digital baseband signal and beamforming information. Considering the single stream transmission, each reflecting element reflects the same symbol in a symbol duration. Thus, we further express the reflection coefficient vector as

$$\boldsymbol{\theta} = [e^{j\psi_1}, \dots, e^{j\psi_n}, \dots, e^{j\psi_N}]^T e^{j\varphi} = \boldsymbol{\psi}s, \quad (9)$$

where $\psi_n = \theta_n - \varphi$. It can be observed that, $\boldsymbol{\psi}$ can function as the beamforming vector to maximize the received SNR, while $s = e^{j\varphi}$ can be viewed as a virtual signal modulated by MPSK.

It is assumed that the channel state information (CSI) is available to the Tx and Rx by using existing channel estimation methods [13]. Thus, in the ideal case where the reflection coefficients of RIS can be continuously adjusted, the optimal beamforming vector can be solved by the maximum-ratio transmission (MRT) [14], i.e.,

$$\tilde{\boldsymbol{\psi}} = [e^{-j\phi_1}, \dots, e^{-j\phi_n}, \dots, e^{-j\phi_N}]^T, \quad (10)$$

which means that the phase shifts induced by channel transmission can be compensated perfectly by beamforming.

On the other hand, the virtual M -ary signal s is generated by the mapping of digital baseband signals on the signal constellation diagram. Without loss of generality, the set of phase of signal modulated by MPSK can be written as

$$\mathcal{S} = \left\{ 0, \frac{2\pi}{M}, \dots, \frac{M-1}{M}2\pi \right\}. \quad (11)$$

Therefore, by combining (9) and (10), the optimal reflection coefficient vector can be denoted as

$$\tilde{\boldsymbol{\theta}} = [e^{j(\varphi-\phi_1)}, \dots, e^{j(\varphi-\phi_n)}, \dots, e^{j(\varphi-\phi_N)}]^T. \quad (12)$$

Correspondingly, the optimal phase shifts of the n -th element can be formulated as

$$\tilde{\theta}_n = \varphi - \phi_n. \quad (13)$$

Due to the hardware limitation, the RIS made of PIN diodes can only take a finite number of discrete phase shifts, which are equally spaced in $[0, 2\pi)$. Therefore, the quantization error will induce for practical implementation. To minimize the quantization error, the discrete phase shifts can be formulated by quantifying the continuous phase shifts to their nearest

points in \mathcal{R} . Consequently, we have

$$\hat{\theta}_n = \arg \min_{\theta \in \mathcal{R}} |\theta - \tilde{\theta}_n|. \quad (14)$$

Since this quantization may lead to unexpected signal phase shifts, in order to successfully recover the signal, the proposed transmitter must satisfy the hardware constraint in the following remark.

Remark The different transmitted symbols are required to correspond to the different reflection phase shifts of RIS. It indicates the number of elements in \mathcal{R} must be no less than the number of elements in \mathcal{S} , i.e. $K \geq M$.

The whole signal transmission steps can be summarized as: (a) obtain the beamforming information according to the known CSI; (b) add the digital baseband and beamforming information to get a digital control signal bit stream (0110...), which corresponds to the bias voltage (LOW, HIGH, HIGH, LOW...); (c) adjust the reflection coefficients of RIS elements via bias voltage; and (d) modulate the carrier signal once arriving the RIS.

III. SIGNAL DEMODULATION AND PERFORMANCE ANALYSIS

By down-converting the received signal and sampling at the optimal sampling moment, the equivalent baseband signal can be obtained as

$$r = \sqrt{P}\mathbf{h}\boldsymbol{\psi}s + w, \quad (15)$$

where $w \sim \mathcal{CN}(0, \sigma^2)$ denotes the noise with the average power σ^2 .

The quantization error between the practical reflection phase and the ideal reflection phase induces additional SNR loss and unexpected phase shifts of the received signal. However, with the available CSI and the phase quantization method, the receiver can compensate for the phase shifts caused by quantization and further recover the received symbols. It means that our proposed transmitter can cooperate with the conventional receiver to accomplish the wireless communication task. Furthermore, we can apply conventional signal demodulation methods to demodulate the received signal. For the analysis convenience, we adopt the zero-forcing (ZF) receiver. Thus, the demodulated signal can be expressed as

$$s' = s + \frac{w}{\sqrt{P}\mathbf{h}\boldsymbol{\psi}}. \quad (16)$$

It should be emphasized that (16) holds only if the quantization levels are greater than or equal to the modulation order. Moreover, the SNR is formulated as

$$\text{SNR} = \frac{\mathbb{E}\{|s|^2\}}{\mathbb{E}\left\{\left|\frac{w}{\sqrt{P}\mathbf{h}\boldsymbol{\psi}}\right|^2\right\}} = \frac{P\mathbb{E}\{|\mathbf{h}\boldsymbol{\psi}|^2\}}{\sigma^2}. \quad (17)$$

Since the beamforming vector $\boldsymbol{\psi}$ can only take a finite number of discrete values, the quantization errors $\theta_n = \hat{\theta}_n - \tilde{\theta}_n$ are inde-

pendently and uniformly distributed in $[-\frac{\pi}{K}, \frac{\pi}{K})$. Therefore, the received SNR can be rewritten as

$$\begin{aligned} \text{SNR} &= \frac{P\mathbb{E}\left\{\left|\sum_{n=1}^N \eta|h_n|e^{j\bar{\theta}_n}\right|^2\right\}}{\sigma^2} \\ &= \frac{P\eta^2}{\sigma^2}\mathbb{E}\left\{\sum_{n=1}^N |h_n|^2 + \sum_{n=1}^N \sum_{i \neq n}^N |h_i||h_n|e^{j\bar{\theta}_n - j\bar{\theta}_i}\right\} \\ &= \frac{P\eta^2}{\sigma^2}\left[N + \frac{\pi}{4}(N^2 - N)\left(\frac{\sin \frac{\pi}{K}}{\frac{\pi}{K}}\right)^2\right]. \end{aligned} \quad (18)$$

If the number of reflection elements N is sufficiently large, the asymptotic SNR can be approximated as

$$\text{SNR} \cong \frac{P\pi\eta^2 N^2}{4\sigma^2} \left(\frac{\sin \frac{\pi}{K}}{\frac{\pi}{K}}\right)^2. \quad (19)$$

It can be observed that SNR is approximately proportional to N^2 . Moreover, SNR improves with the increase of quantization levels K and approaches optimal value when $K \rightarrow \infty$ (i.e., ideal continuous phase shifts).

Since the received signal of the considered communication system has the same mathematical expression with conventional one, our proposed transmitter has the same BER performance as a conventional transmitter under the same SNR condition. Consequently, according to the generalized BER expression of MPSK in [15], we have

$$\text{BER} \cong \begin{cases} \frac{\text{erfc}\left(\frac{\sqrt{\text{SNR}} \sin \frac{\pi}{M}}{\log_2 M}\right)}{\log_2 M} & \text{if } M \geq 4, \\ \frac{1}{2} \text{erfc}\sqrt{\text{SNR}} & \text{if } M = 2, \end{cases} \quad (20)$$

where $\text{erfc}(\cdot)$ is the complementary error function as

$$\text{erfc}(x) = \frac{2}{\sqrt{\pi}} \int_x^\infty e^{-z^2} dz. \quad (21)$$

After substituting (19) into (20), we have

$$\text{BER} \cong \begin{cases} \frac{\text{erfc}\left(\mu N \left(\frac{\sin \frac{\pi}{K}}{\frac{\pi}{K}}\right) \sin \frac{\pi}{M}\right)}{\log_2 M} & \text{if } M \geq 4, \\ \frac{1}{2} \text{erfc}\left(\mu N \left(\frac{\sin \frac{\pi}{K}}{\frac{\pi}{K}}\right)\right) & \text{if } M = 2, \end{cases} \quad (22)$$

where $\mu = \frac{\sqrt{P\pi}}{2\sigma}$. Although the SNR loss caused by quantization error increases the BER, it can be compensated by increasing the number of reflecting elements. More importantly, the proposed RIS-based transmitter trades the performance loss for RF chain-free, low-cost digital modulation and transmission.

IV. SIMULATION RESULTS

In this section, we provide simulation results to validate the performance of our proposed transmitter design. Moreover, we compare the theoretical analysis results, which are obtained through derived expression, with Monte Carlo simulation results, which are the exact counts of SNR and BER. The path loss at the reference distance of 1 m, the path loss exponent for the channel from the RIS to the RX, and the average noise power are set as $\rho = -20$ dB, $\alpha = 2.8$ and $\sigma^2 = -70$ dBm, respectively, which are consistent with the sets in [13]. The distance between the feed antenna and the

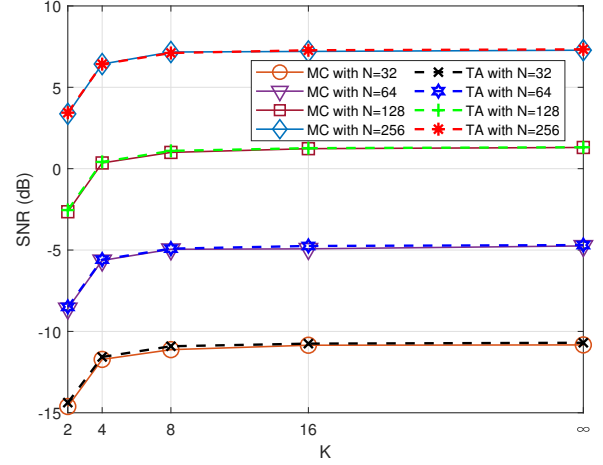


Fig. 2. SNR performance versus phase quantization levels with transmit power $P = -20$ dBm and modulation orders $M = 2$.

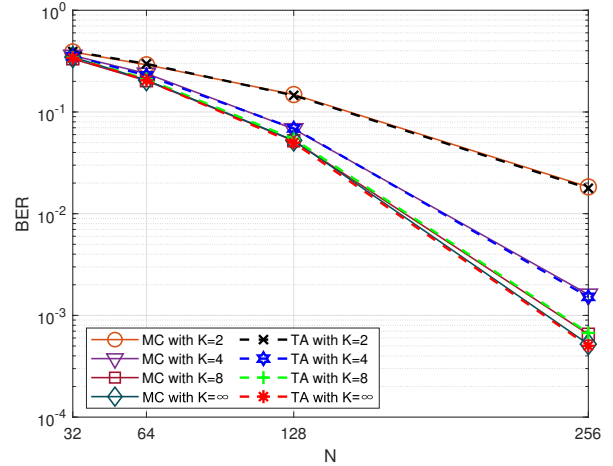


Fig. 3. BER performance versus the number of reflecting elements with transmit power $P = -20$ dBm and modulation orders $M = 2$.

RIS, and the distance between the RIS and the Rx are set as $d = 1$ m and $D = 60$ m, respectively.

To validate the theoretical analysis results, we compare the SNR and BER of Monte Carlo (MC) simulation results and theoretical analysis (TA) results in Figs. 2 and 3, respectively. It is shown that the theoretical analysis results for both SNR and BER coincide well with Monte Carlo simulation results regardless of the quantization levels and the number of reflecting elements. This supports the validity of our theoretical analysis.

Fig. 2 shows the SNR performance versus the phase quantization levels at the RIS, where the numbers of reflecting elements $N \in \{32, 64, 128, 256\}$. From Fig. 2, it is observed that as quantization level K increases from 2 to 4, the SNR performance significantly improves, while the improvement from 4 to 16 is quite slight. Furthermore, there is little SNR performance gap between $K = 16$ and $K = \infty$ (i.e., the ideal continuous phase shifts). It indicates that excessive quantifica-

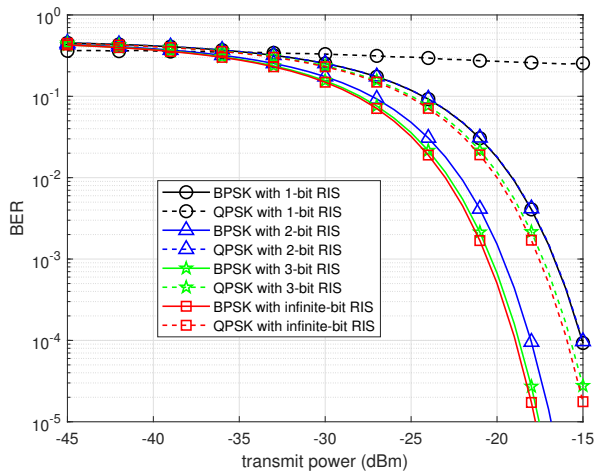


Fig. 4. BER performance by different bit RIS-based transmitter versus transmit power with the number of reflecting elements $N = 256$.

tion levels bring limited improvement of SNR performance but higher hardware cost. As shown in Fig. 3, the BER decreases significantly as the number of reflecting elements increases. In contrast, increasing the quantization levels brings a relatively limited reduction of BER. In other words, compared to K , N is more influential in the improvement of SNR and BER. Therefore, in most application scenarios, as the requirements of SNR and BER are developed, it is more efficient to implement more reflecting elements instead of increasing the quantization levels.

As illustrated in Fig. 4, if baseband signals are modulated by BPSK or QPSK, the BER performance of demodulated signal with different transmit power is measured. When the baseband signal is modulated by QPSK and transmitted by 1-bit RIS, the BER is high and independent of transmit power, because 1-bit RIS can only induce 2 different phase states and fails to achieve QPSK modulation. Furthermore, we can observe that the finite-bit RIS suffers the BER loss compared to the case with infinite-bit RIS, because the phase quantization error results in the loss of SNR. However, as the quantization level increases, the performance gap rapidly decreases and becomes nearly negligible. It verifies that the proposed finite-bit RIS-based transmitter has comparable performance compared with the infinite-bit RIS-based transmitter. Additionally, there is a trade-off between spectrum efficiency and energy efficiency, since increasing the number of reflecting elements and phase quantization levels improves the communication performance, but brings higher hardware cost and power consumption.

V. CONCLUSION

In this letter, a cost-efficient RIS-assisted transmitter design with discrete phase shifts is proposed. The SNR and BER performance was evaluated and verified with both theoretical analysis and simulations. The results revealed that the proposed transmitter design can approach similar communication performance with lower hardware complexity, making it superior to the existing designs. In addition, we demonstrated that

the SNR and BER loss caused by phase quantization error can be compensated by increasing the number of reflecting elements. Moreover, the proposed design avoids the need for complex DSP hardware and costly RF chains, to achieve reliable digital modulation and signal transmission, which provides an efficient solution for future wireless communication networks.

REFERENCES

- [1] F. Sofrabi and W. Yu, "Hybrid digital and analog beamforming design for large-scale antenna arrays," *IEEE J. Sel. Topics Signal Process.*, vol. 10, no. 3, pp. 501–513, Apr. 2016.
- [2] M. A. ElMossallamy, H. Zhang, L. Song, K. G. Seddik, Z. Han, and G. Y. Li, "Reconfigurable intelligent surfaces for wireless communications: Principles, challenges, and opportunities," *IEEE Trans. Cognit. Commun. Netw.*, vol. 6, no. 3, pp. 990–1002, Sep. 2020.
- [3] Q. Wu, S. Zhang, B. Zheng, C. You, and R. Zhang, "Intelligent reflecting surface-aided wireless communications: A tutorial," *IEEE Trans. Commun.*, vol. 69, no. 5, pp. 3313–3351, May 2021.
- [4] C. Huang, A. Zappone, G. C. Alexandropoulos, M. Debbah, and C. Yuen, "Reconfigurable intelligent surfaces for energy efficiency in wireless communication," *IEEE Trans. Wireless Commun.*, vol. 18, no. 8, pp. 4157–4170, Aug. 2019.
- [5] M. Di Renzo, A. Zappone, M. Debbah, M.-S. Alouini, C. Yuen, J. de Rosny, and S. Tretyakov, "Smart radio environments empowered by reconfigurable intelligent surfaces: How it works, state of research, and the road ahead," *IEEE J. Sel. Areas Commun.*, vol. 38, no. 11, pp. 2450–2525, Nov. 2020.
- [6] H. Guo, Y.-C. Liang, J. Chen, and E. G. Larsson, "Weighted sum-rate maximization for reconfigurable intelligent surface aided wireless networks," *IEEE Trans. Wireless Commun.*, vol. 19, no. 5, pp. 3064–3076, May 2020.
- [7] B. Di, H. Zhang, L. Song, Y. Li, Z. Han, and H. V. Poor, "Hybrid beamforming for reconfigurable intelligent surface based multi-user communications: Achievable rates with limited discrete phase shifts," *IEEE J. Select. Areas Commun.*, vol. 38, no. 8, pp. 1809–1822, Aug. 2020.
- [8] Y. Lu, M. Hao, and R. Mackenzie, "Reconfigurable intelligent surface based hybrid precoding for THz communications," *Intelligent and Converged Networks*, vol. 3, no. 1, pp. 103–118, Mar. 2022.
- [9] J. Zhao, X. Yang, J. Y. Dai, Q. Cheng, X. Li, N. H. Qi, J. C. Ke, G. D. Bai, S. Liu, S. Jin, A. Alù, and T. J. Cui, "Programmable time-domain digital-coding metasurface for non-linear harmonic manipulation and new wireless communication systems," *Nat. Sci. Rev.*, vol. 6, no. 2, pp. 231–238, Mar. 2019.
- [10] W. Tang, X. Li, J. Y. Dai, S. Jin, Y. Zeng, Q. Cheng, and T. J. Cui, "Wireless communications with programmable metasurface: Transceiver design and experimental results," *China Commun.*, vol. 16, no. 5, pp. 46–61, May 2019.
- [11] W. Tang, J. Y. Dai, M. Z. Chen, K.-K. Wong, X. Li, X. Zhao, S. Jin, Q. Cheng, and T. J. Cui, "MIMO transmission through reconfigurable intelligent surface: System design, analysis, and implementation," *IEEE J. Sel. Areas Commun.*, vol. 38, no. 11, pp. 2683–2699, Nov. 2020.
- [12] L. Dai, B. Wang, M. Wang, X. Yang, J. Tan, S. Bi, S. Xu, F. Yang, Z. Chen, M. D. Renzo, C.-B. Chae, and L. Hanzo, "Reconfigurable intelligent surface-based wireless communications: Antenna design, prototyping, and experimental results," *IEEE Access*, vol. 8, pp. 45913–45923, 2020.
- [13] J. An, C. Xu, L. Gan, and L. Hanzo, "Low-complexity channel estimation and passive beamforming for RIS-assisted MIMO systems relying on discrete phase shifts," *IEEE Trans. Commun.*, vol. 70, no. 2, pp. 1245–1260, Feb. 2022.
- [14] T. Lo, "Maximum ratio transmission," *IEEE Trans. Commun.*, vol. 47, no. 10, pp. 1458–1461, Oct. 1999.
- [15] J. Lu, K. Letaief, J.-I. Chuang, and M. Liou, "M-PSK and M-QAM BER computation using signal-space concepts," *IEEE Trans. Commun.*, vol. 47, no. 2, pp. 181–184, Feb. 1999.